Computational and dynamic performance of NN-based control in wind energy systems

Imodane Belkasem [1*], *Dahmane* Kaoutar[1], *Bouachrine* Brahim[1], *El idrissi* Abdellah[1], *Benydir* Mohamed[1], and *Ajaamoum* Mohamed[1]

[1]Laboratory of Engineering Sciences and Energy Management (LASIME), Ibn Zohr University, National School of Applied Sciences, Agadir, Morroco.

Abstract. In modern power grids, the integration of renewable energy sources such as wind power is crucial to achieving sustainable energy goals. However, the intermittent nature of renewable energy generation creates grid stability issues, particularly with the stabilization of the DC link voltage in systems using Permanent Magnet Synchronous Generators (PMSGs). This paper investigates the effectiveness of a boost converter combined with Neural Network Control (NNC) trained by Sliding Mode Control (SMC) in managing voltage fluctuations. To achieve this, we implement both control strategies on a LAUNCHXL-F28069M DSP board using Processor-In-the-Loop (PIL) techniques, enabling a direct comparison of their dynamic and computational performance. While NNC-based control shows superior adaptability and responsiveness, it consumes more computational resources than SMC, particularly in terms of execution time and power consumption. This study provides an overview of the trade-offs between resource consumption and performance, offering a clearer understanding of control strategies for optimizing renewable energy management in embedded systems.

Keywords—Sliding Mode Control, Neural Network Control, Processor In the Loop, Wind turbine, DC/DC Converter.

1 Introduction

The integration of renewable energy sources into power systems has become increasingly important in the face of global challenges related to climate change, energy security, and the growing exploitation of fossil fuels [1]. This transition to renewable energies aims not only to reduce greenhouse gas emissions but also to diversify energy supplies, enhance energy security, and promote economic development in local communities [3]. Among the various renewable energy sources, wind power has proved to be one of the most promising due to its wide availability and scalability potential [2]. As countries work to achieve ambitious sustainable development objectives, the role of wind power is set to grow considerably, requiring improvements in the efficiency and reliability of the power electronic systems that facilitate its integration into existing grids.

Wind energy conversion systems (WECS) are essential for converting the wind's kinetic energy into electrical energy [4]. These systems often use permanent magnet synchronous generators (PMSGs), which offer several advantages, including high efficiency, compact size, and reduced maintenance requirements compared to doubly-fed induction generators (DFIG) [5]. However, integrating PMSGs into power grids presents challenges, particularly with the importance of stabilizing the DC link voltage, which is crucial for maintaining optimum grid-side inverter performance [6]. The DC link acts as a bridge between the generator and the inverter, enabling a smooth transfer of energy and regulating voltage levels. Fluctuations in the DC link voltage can lead to instability of the inverter output, resulting in poor power quality and potentially affecting the overall reliability of the power system [6].

One of the most critical issues facing wind power systems is the intermittent and fluctuating nature of renewable energy production [7]. Wind power generation is inherently variable due to changes in wind speed, wind direction, and turbulence. These fluctuations can cause significant problems for grid stability, requiring the implementation of effective control strategies to manage voltage fluctuations and ensure robust system performance [7]. Various control strategies have been developed to meet these challenges, with Sliding Mode Control (SMC) being one of the most widely adopted methods [8].

SMC offers robustness to system disturbances, making it an appropriate choice for applications where uncertainty and variability are predominant. SMC works by adjusting the control input to drive the system state towards a predefined sliding surface, ensuring stable operation despite external disturbances. This control method has been successfully applied in many power electronics applications, demonstrating its effectiveness in improving system stability and performance [8].

The increasing complexity of power grids has resulted in a growing interest in adaptive control methods, particularly those based on Neural Network Controls (NNCs) [9]. NNCs have attracted attention due to their ability to learn and adapt to varying system

* Corresponding author: b.imodane@uiz.ac.ma

parameters, enabling them to effectively manage the dynamic nature of wind power generation [10]. These networks can model complex nonlinear relationships between input and output variables, improving control performance in situations where traditional methods may prove ineffective [10]. The focus is on the computational burden, particularly in terms of execution time and power consumption, when these control methods are implemented on DSP boards.

Many studies have explored the role of various control strategies in stabilizing the DC link voltage for PMSG systems [11,12,13]. Research indicates that SMC, in particular, can effectively handle voltage fluctuations in dynamic environments, making it a suitable choice for the control of PMSG-based wind power systems [14]. Additionally, adaptive control using NNCs has been applied in various fields of power electronics, showing potential for improving system performance in dynamic environments [15]. However, the computational complexity of NNC-based control, particularly in real-time applications on DSP platforms, has not yet been fully addressed, necessitating further research into its practicality.

In [16], to evaluate the computational efficiency and dynamic performance of the proposed control methods, a boost converter is used to regulate the DC link voltage in a wind power system. The choice of a boost converter is based on its ability to increase the input voltage, helping to maintain the desired DC link voltage despite fluctuations in wind power generation. The use of a boost converter in combination with NN-based adaptive controllers presents a promising approach to improving the stability and performance of wind energy systems.

This work will involve the use of SMC to train adaptive NN-based controllers, which will then be compared with traditional SMC methods. Dynamic performance is a very important aspect of this study, as it refers to the efficiency with which the control system responds to changes or disturbances in real time. In power electronics and renewable energy systems, dynamic performance includes the system's ability to adapt to fluctuations in wind power generation, to maintain stability in the event of sudden load changes, and to manage non-linearities. The responsiveness of the boost converter, controlled by SMC or NNC, to these fluctuations is essential for evaluating system stability and performance. In addition, minimizing overshoot, settling time, and ensuring rapid restoration after disturbances are essential elements of dynamic performance. The primary objective is to evaluate the performance of NN-based control compared with SMC, particularly in terms of responsiveness, adaptability, and energy efficiency. Key performance metrics, such as execution time and energy consumption were measured to assess the computational overhead and dynamic performance introduced by NNC-based controllers.

This paper is organized as follows: the second section covers the design and mathematical analysis of the DC/DC power converter in continuous conduction mode. The third section presents the modeling of the converter. The fourth section describes the proposed control strategies. The fifth section provides an overview of the PIL testing. The sixth section presents the results of implementing SMC and Adaptive NNC using the PIL technique. Finally, concluding remarks and suggestions for future research are discussed in the last section.

2 Sizing of boost converter

In renewable energy systems, like wind power applications, the management and regulation of the output voltage is very important. This is usually done using a conventional non-isolated boost converter, as shown in Figure 1. The boost converter consists of several essential components, including a DC voltage source (Vin), a controlled switch (S), an inductor (L), a diode (D), a filter capacitor (C) and a load, as shown in Figure 2. Our study will focus on the converter's performance in continuous conduction mode (CCM), examining different operational states as a function of the position of the S switch.

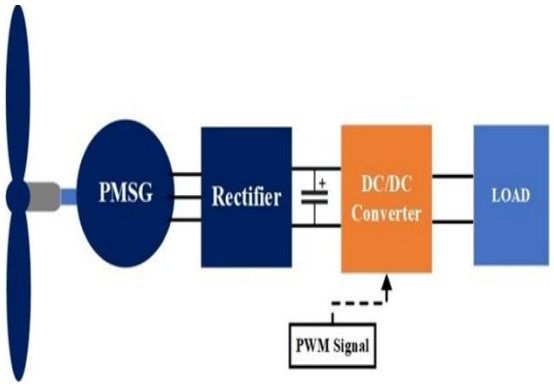

Fig. 1. Boost converter integration in wind turbine system.

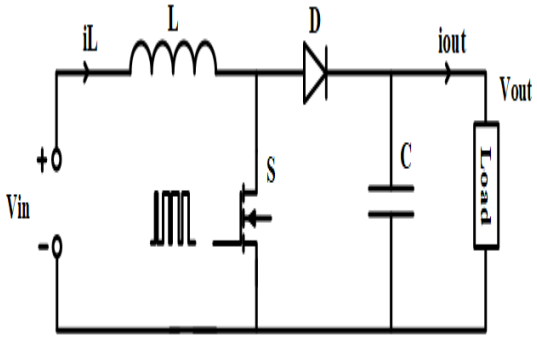

Fig. 2. Electrical schematic of the DC/DC boost converter.

The ripple current ΔI_L is typically set to 10% of the current passing through the inductor L [17]. The duty cycle (α) of the power converter is determined using the formula (1) where V_{in} and V_{out} represent the input voltage and the output voltage of the converter, respectively:

$$\alpha = \frac{V_{out} - V_{in}}{V_{out}} \quad (1)$$

The value of L is determined using the expression below (2), where f is the switching frequency.

$$L = \frac{\alpha \times V_{in}}{f \times \Delta I_L} \quad (2)$$

For the capacitor C, its value is calculated as:

$$C = \frac{\alpha \times I_{out}}{f \times \Delta V_{out}} \quad (3)$$

Where ΔV_{out} represent the ripple output voltage, typically 1% of V_{out} [17] and I_{out} is the current passing through the load.

Table 1 shows the main parameters of the DC/DC boost converter used in this study [18]. These parameters are essential for boosting the input voltage to the desired output voltage level.

Table 1. Main parameters of the DC/DC boost converter

Parameter	Value
Vin	12V
Vout	24 V
C	600 µF
L	220 µH
F	45 kHz
R	100 Ω

3 Modeling of boost converter

A boost power converter is a type of converters that boosts the input dc voltage. To understand its operation, we analyze its states when the switch is ON (closed) and OFF (Open).

when the switch is ON:

$$\frac{di_L}{dt} = \frac{1}{L} V_{in} \quad (4)$$

$$\frac{dV_{out}}{dt} = \frac{1}{C} * \left(-\frac{V_{out}}{R} \right) \quad (5)$$

And when the switch is OFF:

$$\frac{di_L}{dt} = \frac{1}{L} * (V_{in} - V_{out}) \quad (6)$$

$$\frac{dVout}{dt} = \frac{1}{C} * \left(i_L - \frac{Vout}{R} \right) \quad (7)$$

The state equations for a boost converter during ON state can be given as equation (8) where i_L represent inductor current:

$$\begin{bmatrix} \frac{di_L}{dt} \\ \frac{dV_{out}}{dt} \end{bmatrix} = \begin{bmatrix} 0 & 0 \\ 0 & -\frac{1}{RC} \end{bmatrix} \begin{bmatrix} i_L \\ V_{out} \end{bmatrix} + \begin{bmatrix} \frac{1}{L} \\ 0 \end{bmatrix} V_{in} \quad (8)$$

And when the switch S is OFF, the state equations can be written as follows:

$$\begin{bmatrix} \frac{di_L}{dt} \\ \frac{dVout}{dt} \end{bmatrix} = \begin{bmatrix} 0 & -\frac{1}{L} \\ \frac{1}{C} & -\frac{1}{RC} \end{bmatrix} \begin{bmatrix} i_L \\ V_{out} \end{bmatrix} + \begin{bmatrix} \frac{1}{L} \\ 0 \end{bmatrix} V_{in} \quad (9)$$

In order to obtain a converter model over a switching period, the state-space averaging technique is used. This technique is based on replacing the state space that approximates the circuit's behavior over the entire period T with a state space that captures the circuit's dynamics accurately over a single switching period [19]. The resulting modified averaged model derived from this technique, is represented by the following formula:

$$A = A_1 \times \alpha + A_2(1 - \alpha) \quad (10)$$

$$B = B_1 \times \alpha + B_2(1 - \alpha) \quad (11)$$

A1, A2, B1 and B2 can be writing as:

$$A_1 = \begin{bmatrix} 0 & 0 \\ 0 & \frac{-1}{RC} \end{bmatrix} \qquad A_2 = \begin{bmatrix} 0 & \frac{-1}{L} \\ \frac{1}{C} & \frac{-1}{RC} \end{bmatrix} \quad (12)$$

$$B_1 = \begin{bmatrix} \frac{1}{L} \\ 0 \end{bmatrix} \qquad B_2 = \begin{bmatrix} \frac{1}{L} \\ 0 \end{bmatrix} \quad (13)$$

Using Eq. (10) and Eq. (11) to get the average space state model of the power converter over the entire period T.

$$\begin{bmatrix} \frac{di_L}{dt} \\ \frac{dV_{out}}{dt} \end{bmatrix} = \begin{bmatrix} 0 & -\frac{(1-\alpha)}{L} \\ \frac{(1-\alpha)}{C} & -\frac{1}{RC} \end{bmatrix} \begin{bmatrix} i_L \\ V_{out} \end{bmatrix} + \begin{bmatrix} \frac{1}{L} \\ 0 \end{bmatrix} V_{in} \quad (14)$$

The state vector is defined as:

$$x = [i_L \quad V_{out}]^T \quad (15)$$

The equation (15) can be presented as follows:

$$\dot{x} = Ax + BV_{in} \quad (16)$$

$$Y = Nx \quad (17)$$

Where Y represent the output vector and:

$$A = \begin{bmatrix} 0 & -\frac{(1-\alpha)}{L} \\ \frac{1-\alpha}{C} & -\frac{1}{RC} \end{bmatrix} \quad B = \begin{bmatrix} \frac{1}{L} \\ 0 \end{bmatrix} \quad N = [0 \quad 1]$$

4 Controller design

4.1 Sliding mode control

Sliding mode control (SMC) is a robust non-linear control strategy for managing the complex dynamics of variable-structure systems. It offers important advantages by guaranteeing system stability and robustness, even in the face of large parameter variations. The SMC approach comprises two distinct methodologies. This paper focuses on the approach mode, in which the control law is designed to steer the state of the system along a predetermined trajectory in state space, thus achieving the desired system behavior in a finite amount of time [20].

The state variables of the system are given as:

$$X = \begin{bmatrix} X_1 \\ X_2 \\ X_3 \end{bmatrix} = \begin{bmatrix} V_{ref} - (Beta * V_{out}) \\ \frac{d}{dt}(V_{ref} - (Beta * V_{out})) \\ \int V_{ref} - (Beta * V_{out})\ dt \end{bmatrix} \quad (18)$$

X_1, X_2 and X_3 represent the voltage error, the derivative of the error, and the integral of the error, respectively. V_{ref} and Beta represent the reference voltage and the voltage divider ratio relative to the converter output. According to equations (8), (9) and (15), equation (18) can be re-expressed as follows:

$$X = \begin{bmatrix} X_1 \\ X_2 \\ X_3 \end{bmatrix} = \begin{bmatrix} V_{ref} - (Beta * V_{out}) \\ \frac{(Beta * V_{out})}{RC} + \frac{Beta}{LC}\int (V_{ref} - V_{in})\bar{\alpha}\ dt \\ \int V_{ref} - (Beta * V_{out})\ dt \end{bmatrix} \quad (19)$$

The control system's state equations in vector space can be expressed as follows:

$$\begin{bmatrix} \dot{X}_1 \\ \dot{X}_2 \\ \dot{X}_3 \end{bmatrix} = \begin{bmatrix} 0 & 1 & 0 \\ 0 & -\frac{1}{RC} & 0 \\ 1 & 0 & 0 \end{bmatrix} \begin{bmatrix} X_1 \\ X_2 \\ X_3 \end{bmatrix} + \begin{bmatrix} 0 \\ \frac{(Beta * V_{out})}{RC} - \frac{(Beta * V_{in})}{LC} \\ 0 \end{bmatrix} \quad (20)$$

The switching function is indicated by the SMC law as shown below:

$$u = \begin{cases} 1, & \gamma > 0 \\ 0, & \gamma < 0 \end{cases} \quad (21)$$

Where γ represents the instantaneous state trajectory, defined as:

$$\gamma = X_1\alpha_1 + X_2\alpha_2 + X_3\alpha_3 = J^T X \quad (22)$$

This equation represents the sliding coefficients.

Where: $J^T = [\alpha_1\ \alpha_2\ \alpha_3]$

To operate the switch S in a converter using Pulse Width Modulation (PWM), a control signal Vc is compared with a sawtooth reference signal Vr. The sawtooth waveform has a linear ramp that rises gradually and then falls sharply, making this comparison effective for establishing the desired duty cycle of the PWM signal, as shown in Figure 3. This comparison produces an equivalent control signal u_{eq}. which is then processed by a PWM modulator to produce the duty cycle. The resulting duty cycle determines the ON/OFF time ratio of the switch S.

$$\dot{\gamma} = J^T AX + J^T B\bar{u}_{eq} = 0 \quad (23)$$

Where $\bar{u}_{eq} = -[J^T B]^{-1} J^T AX \quad (24)$

$$\bar{u}_{eq} = \frac{Beta * L * \left(\frac{\alpha 1}{\alpha 2} - \frac{1}{RC}\right)}{Beta * (V_{out} - V_{in})} Ic - \frac{\alpha 3 * L * C * (Vref - Beta * V_{out})}{\alpha 2 * Beta(V_{out} - V_{in})} \quad (25)$$

For the equation (25), $0 < \bar{u}_{eq} < 1$ by taking into account:

$$\bar{u}_{eq} = 1 - u_{eq} \quad (26)$$

Equation (25) can be described briefly as follows:

$$u_{eq} = \frac{-Ic * Beta * L * \left(\frac{\alpha 1}{\alpha 2} - \frac{1}{RC}\right) + \frac{\alpha 3 * L * C}{\alpha 2} * (Vref - Beta * V_{out}) + Beta * (V_{out} - V_{in})}{Beta * (V_{out} - V_{in})} \quad (27)$$

Where $0 < u_{eq} < 1$

In a similar expression:

$$u_{eq} = \frac{-KP_1 * ic + KP_2(V_{ref} - Beta * V_{out}) + Beta * (V_{out} - V_{in})}{Beta(V_{out} - V_{in})} \quad (28)$$

$$0 < u_{eq} = \frac{Vc}{Vr} < 1 \quad (29)$$

Where

$$KP_1 = Beta * \left(\frac{\alpha 1}{\alpha 2} - \frac{1}{RC}\right)$$

$$KP_2 = \frac{\alpha 3}{\alpha 2} * L * C$$

$$Vr = Beta * (V_{out} - V_{in})$$

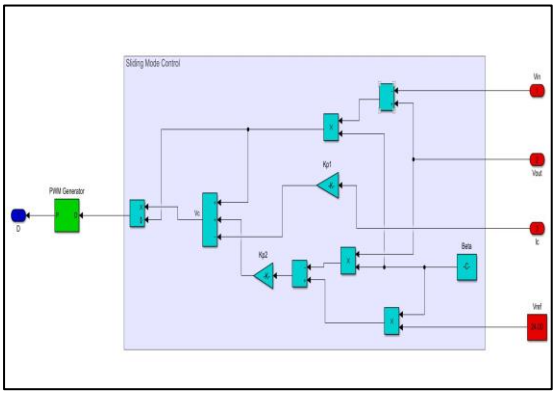

Fig. 3 Simulation model of the controlled system with SMC.

4.2 Neural Network Controller

Artificial Neural Networks (ANNs) are recognized for their ability to solve complex problems without needing detailed system information. They learn the relationship between input and output variables through previously recorded data and can effectively handle large, complex systems with numerous parameters. Trained ANNs can approximate arbitrary input-output mappings. In our system, we use the same inputs as Sliding Mode Control (SMC)—specifically, Ic, Vin, Vout and Vref—to train our model, which outputs the

duty cycle as shown in Figure 4. This output is then used to control the boost converter after converte it to a PWM signal. We utilize 16 hidden neurons and the Levenberg-Marquardt training algorithm for our model.

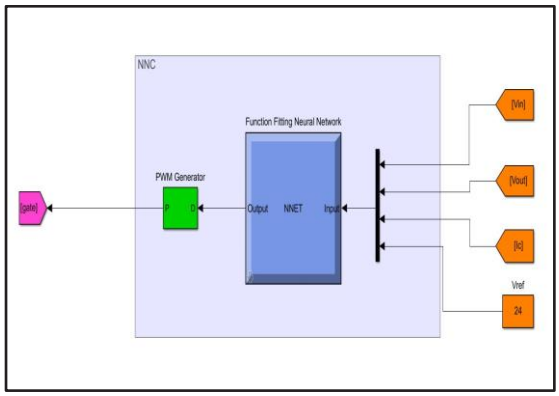

Fig. 4. Simulation model of the controlled system with NNC.

5 Processor-In-The-Loop testing

Processor-in-the-loop (PIL) prototyping employed in this work is a very effective technique that bridges the gap between virtual simulations and real-world system implementation. It enables control algorithms executed on a physical DSP board to be verified and validated before being integrated into a real electrical system. As shown in Figure 5, The value of PIL prototyping lies in confirming the accuracy of digital control implementations on real microcontrollers, while the power components are simultaneously simulated by a computer. This means that the control part is executed on the board, while the power part is simulated in Matlab/Simulink.

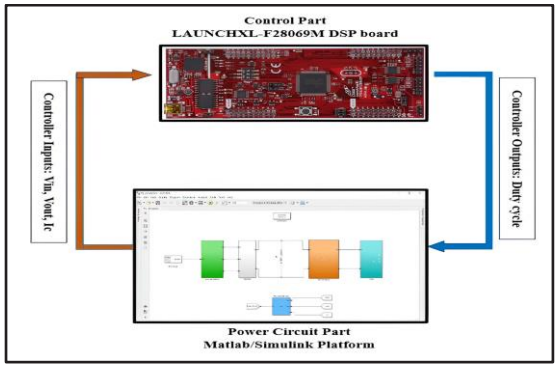

Fig. 5. The representation of the PIL co-simulation setup.

The proposed controllers SMC and NNC were validated using a Processor-in-the-Loop (PIL) test, which utilized MATLAB/Simulink software and the LAUNCHXL-F28069M DSP board, as shown in Figure 6). In this study, the PIL technique is applied to the LAUNCHXL-F28069M board in the following way: first, a control algorithm subsystem is created in Matlab/Simulink to interface with the DSP board, enabling the integrated control algorithm to be executed. The DSP board is then selected as the target model, with the inputs and outputs of the control system defined. The control algorithm is built and uploaded to the DSP board. A USB communication link is set up between the DSP board and Simulink, along with an appropriate time step configuration. Finally, the control model is transferred to the DSP board, with Matlab/Simulink generating the necessary programming code. The control algorithm on the DSP board is then used to run the system via the Matlab/Simulink platform.

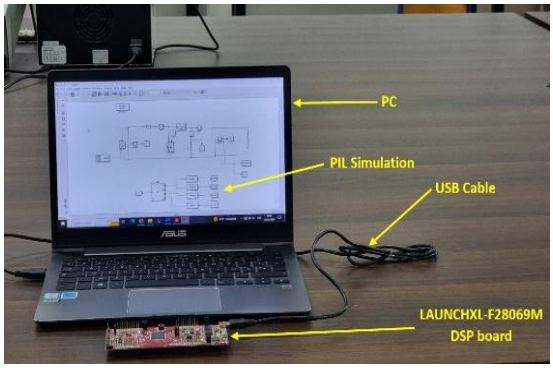

Fig. 6. Processor in the loop platform.

6 Results and discussion

6.1. Dynamic performance results

To evaluate the controller's dynamic performance, key measures are used: output voltage response shows how the voltage adjusts over time, peak overshoot percentage measures the maximum deviation before stabilization, stabilization time evaluates how quickly stabilization takes after a disturbance, and MAPE (Mean Absolute Percentage Error) expresses errors as a percentage of actual values.

$$\text{MAPE} = \frac{1}{N}\sum_{t_0}^{N}\frac{1}{N}\left|\frac{V_{out}-V_{ref}}{V_{out}}\right| * 100 \qquad (30)$$

The Processor-in-the-Loop (PIL) simulation compares the voltage regulation of a boost converter using Sliding Mode Control (SMC) and a Neural Network controller (NNC) trained with SMC. Figure 6 illustrates the input voltage, while Figures 7 and 8 show the performance outcomes, respectively. Both controllers operate on the LAUNCHXL-F28069M DSP board, with the power circuit simulated in Matlab/Simulink. The results show minimal differences, utilizing a variable input voltage profile from a wind turbine and a load change from 100 Ω to 70 Ω at 0.08 s.

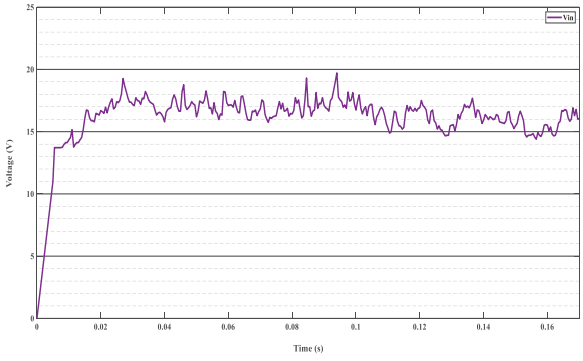

Fig. 7. Input voltage profile.

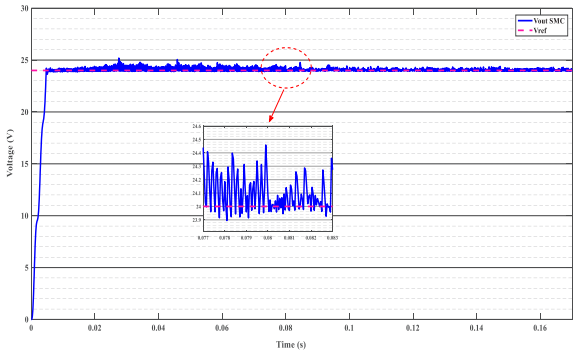

Fig. 8. Output voltage response using SMC.

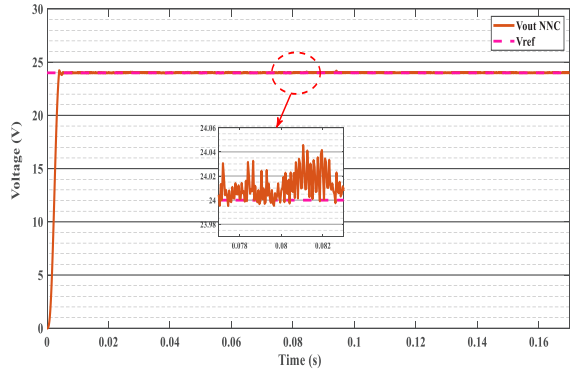

Fig. 9. Output voltage response using NNC.

The comparison between Sliding Mode Control (SMC) and Neural Network Control (NNC) shows that SMC achieves a lower maximum overshoot of 0.49% compared to 0.91% for NNC, meaning it better limits deviations beyond the desired value. However, NNC outperforms SMC in settling time, reaching stability faster at 3.95 ms versus 5.15 ms for SMC. Additionally, NNC has a slightly lower Mean Absolute Percentage Error (MAPE) of 0.37% compared to 0.42% for SMC, indicating more accurate overall performance.

Table 2. The comparative results of dynamic performance using the PIL method

Metric	SMC	NNC
Maximum overshoot	0.49 %	0.91 %
Settling time	5.15 ms	3.95 ms
MAPE	0.42 %	0.37%

6.2. Computational performance results

To identify the optimal controller for hardware implementation, the computational performance and resource utilization of Sliding Mode Control (SMC) and Neural Network Control (NNC) were compared based on execution time and power consumption. Simulations using PIL technique on a DSP board showed that SMC has a shorter execution time (1.43 µs on hardware, 0.76 µs in simulation) compared to NNC (1.93 µs on hardware, 1.7 µs in simulation). SMC also consumed less power (1.30 W) than NNC (1.45 W), making it more suitable for energy-efficient and fast-response applications. Table 3 below summarizes the computational performance of each controller.

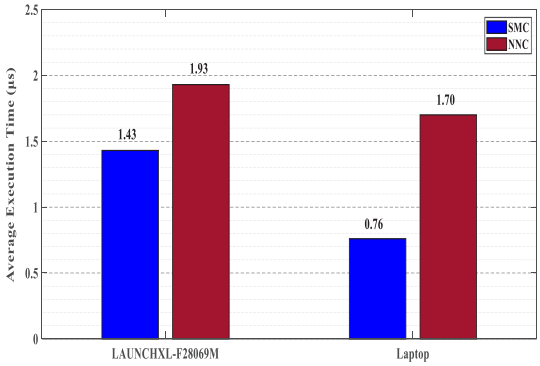

Fig. 10. Execution time of each controller.

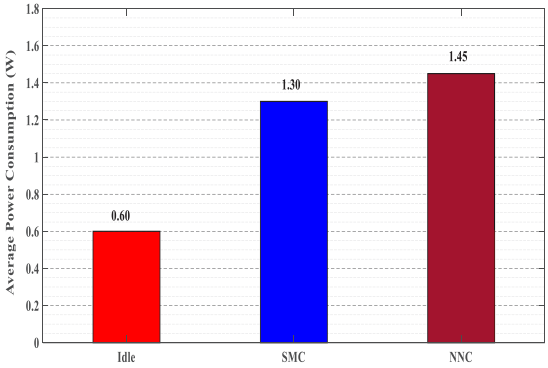

Fig. 11. Power consumption of each controller.

Table 3. Comparative results of computational performance of controllers using PIL

Metric	SMC	NNC
Execution time (DSP)	1.43 µs	1.93 µs
Execution time (Laptop)	0.76 µs	1.7 µs
Power consumption	1.30 W	1.45 W

7 Conclusion

The present study evaluated the performance of Sliding Mode Control (SMC) and neural network control (NNC) for boost DC/DC converters in wind power systems using permanent magnet synchronous generators (PMSGs). The SMC showed superior dynamic performance, with lower maximum overshoot

(0.49%) and slightly longer settling time (5.15 ms), as well as lower error measurements (MAPE: 0.42%). On the other hand, NNC has a higher maximum overshoot (0.91%) but a faster settling time (3.95 ms), with slightly better error performance (MAPE: 0.37%). In terms of computational performance, the SMC demonstrated greater efficiency, with shorter execution times on DSP platforms (1.43 µs) and laptops (0.76 µs), as well as lower power consumption (1.30 W). In contrast, NNCs, while showing adaptability in dynamic performance, had longer execution times on DSPs (1.93 µs) and laptops (1.7 µs), with higher power consumption (1.45 W). Processor-in-the-loop (PIL) validation confirmed these results, showing that the SMC offers better computational and power efficiency, making it more suitable for real-time applications on resource-constrained platforms such as DSP boards. However, NNCs demonstrated better adaptability and faster system response, highlighting their potential for applications that require rapid adjustments to changing system conditions. Future research should focus on reducing the computational requirements of NNCs while maintaining their adaptive capabilities. In addition, hybrid control strategies combining the dynamic performance of SMCs and the adaptability of NNCs could further enhance the efficiency and reliability of power conversion systems in renewable energy applications.

References

[1]. W. Strielkowski, L. Civín, E. Tarkhanova, M. Tvaronavičienė, Y. Petrenko, *Renewable energy in the sustainable development of electrical power sector: A review*. **Energies** 14, 8240 (2021). https://doi.org/10.3390/en14248240

[2]. P. Roy, J. He, T. Zhao, Y. V. Singh, Recent advances of wind-solar hybrid renewable energy systems for power generation: A review. **IEEE Open J. Ind. Electron. Soc**. 3, 81-104 (2022). https://doi.org/10.1109/OJIES.2022.3144093

[3]. M. M. V. Cantarero, *Of renewable energy, energy democracy, and sustainable development: A roadmap to accelerate the energy transition in developing countries*. **Energy Res. Soc. Sci.** 70, 101716 (2020). https://doi.org/10.1016/j.erss.2020.101716

[4]. B. Desalegn, D. Gebeyehu, B. Tamrat, *Wind energy conversion technologies and engineering approaches to enhancing wind power generation: A review*. **Heliyon** 8, 11 (2022). https://doi.org/10.1016/j.heliyon.2022.e11263

[5]. M. M. Mahmoud, M. Khalid Ratib, M. M. Aly, A. M. M. Abdel-Rahim, *Wind-driven permanent magnet synchronous generators connected to a power grid: Existing perspective and future aspects*. **Wind Eng.** 46, 189-199 (2022). https://doi.org/10.1177/0309524X211022728

[6]. M. M. Mahmoud, M. M. Aly, A. M. M. Abdel-Rahim, *Enhancing the dynamic performance of a wind-driven PMSG implementing different optimization techniques*. **SN Appl. Sci.** 2, 1-19 (2020). https://doi.org/10.1007/s42452-020-2439-3

[7]. N. Mlilo, J. Brown, T. Ahfock, *Impact of intermittent renewable energy generation penetration on the power system networks: A review*. **Technol. Econ. Smart Grids Sustain. Energy** 6, 25 (2021). https://doi.org/10.1007/s40866-021-00123-w

[8]. S. J. Gambhire, D. R. Kishore, P. S. Londhe, S. N. Pawar, *Review of sliding mode based control techniques for control system applications*. **Int. J. Dyn. Control** 9, 363-378 (2021). https://doi.org/10.1007/s40435-020-00638-7

[9]. A. Elnozahy, A. M. Yousef, F. K. Abo-Elyousr, M. Mohamed, S. A. M. Abdelwahab, *Performance improvement of hybrid renewable energy sources connected to the grid using artificial neural network and sliding mode control*. **J. Power Electron.** 21, 1166-1179 (2021).https://doi.org/10.1007/s43236-021-00242-8

[10]. M. S. Nazir, F. Alturise, S. Alshmrany, H. M. J. Nazir, M. Bilal, A. N. Abdalla, Z. M. Ali, *Wind generation forecasting methods and proliferation of artificial neural network: A review of five years research trend*. **Sustainability** 12, 3778 (2020). https://doi.org/10.3390/su12093778

[11]. Y. Zhu, Z. Ma, Z. Wang, *An improved fuzzy logic based DC-link voltage control strategy for smoothing output power of the PMSG-WECS*. **Energy Rep.** 8, 8413-8425 (2022). https://doi.org/10.1016/j.egyr.2022.06.049

[12]. B. Majout, H. El Alami, H. Salime, N. Zine Laabidine, Y. El Mourabit, S. Motahhir, B. Bossoufi, *A review on popular control applications in wind energy conversion system based on permanent magnet generator PMSG*. **Energies** 15, 6238 (2022). https://doi.org/10.3390/en15176238

[13]. A. Abedi, B. Rezaie, A. Khosravi, M. Shahabi, *DC-bus Voltage Control based on Direct Lyapunov Method for a Converter-based Stand-alone DC Micro-grid*. **Electric Power Syst. Res.** 187, 106451 (2020). https://doi.org/10.1016/j.epsr.2020.106451

[14]. L. Xiong, P. Li, M. Ma, Z. Wang, J. Wang, *Output power quality enhancement of PMSG with fractional order sliding mode control*. **Int. J. Electr. Power Energy Syst.** 115, 105402 (2020). https://doi.org/10.1016/j.ijepes.2019.105402

[15]. A. N. Akpolat, M. R. Habibi, H. R. Baghaee, E. Dursun, A. E. Kuzucuoğlu, Y. Yang, F. Blaabjerg, *Dynamic stabilization of DC microgrids using ANN-based model predictive control*. **IEEE Trans. Energy Convers.** 37, 999-1010 (2021). https://doi.org/10.1109/TEC.2021.3118664

[16]. M. Amir, A. K. Prajapati, S. S. Refaat, *Dynamic performance evaluation of grid-connected hybrid renewable energy-based power generation for stability and power quality enhancement in smart grid*. **Frontiers Energy Res.** 10, 861282 (2022). https://doi.org/10.3389/fenrg.2022.861282

[17]. V. Y. Xie, V. Adrian, S.-Y. Tay, J. Lee, P. K. Chan, J. Chang, *An Accurate Digital Inductor Current Sensor for Current-Ripple-Based DC-DC Converters*. in **2023 IEEE Int. Symp. Circuits Syst. (ISCAS)**, Monterey, CA, USA (2023), 1-5. https://doi.org/10.1109/ISCAS46773.2023.10181635

[18]. M. BENYDIR, O. M'HAND, S. MOUSLIM, et al., *Implementation and analysis of a fuzzy logic and sliding mode controller on a boost DC/DC converter in a PV array*. **Int. J. Renew. Energy Res.** 13, 294-301 (2023). https://doi.org/10.20508/ijrer.v13i1.13862.g8683

[19]. L. Wu, J. Liu, S. Vazquez, S. K. Mazumder, *Sliding mode control in power converters and drives: A review*. **IEEE/CAA J. Automatica Sinica** 9, 392-406 (2021). https://doi.org/10.1109/JAS.2021.1004380

[20]. S. J. Gambhire, D. R. Kishore, P. S. Londhe, S. N. Pawar, *Review of sliding mode based control techniques for control system applications*. **Int. J. Dyn. Control** 9, 363-378 (2021). https://doi.org/10.1007/S40435-020-00638-7